Computational Materials Science 98 (2015) 51–55

Contents lists available at ScienceDirect

Computational Materials Science

journal homepage: www.elsevier.com/locate/commatsci

Inverse design of materials by multi-objective differential evolution

Yue-Yu Zhang [a], Weiguo Gao [b], Shiyou Chen [a], Hongjun Xiang [a], Xin-Gao Gong [a,*]

[a] Key Laboratory of Computational Physical Sciences (Ministry of Education), State Key Laboratory of Surface Physics, and Department of Physics, Fudan University, Shanghai 200433, PR China
[b] School of Mathematical Science, Fudan University, Shanghai 200433, PR China

ARTICLE INFO

Article history:
Received 25 August 2014
Received in revised form 21 October 2014
Accepted 28 October 2014
Available online 19 November 2014

Keywords:
IM^{2}ODE
Inverse design
Multi-Objective Differential Evolution
Electronic structure
Hardness

ABSTRACT

Inverse design is a promising approach in the realm of material science for finding structures with desired property. We developed a new package with novel algorithm for inverse design named as IM^{2}ODE (inverse design of Materials by Multi-Objective Differential Evolution). The target properties of concern include the optical and electronic-structure properties of semiconductors, hardness of crystals, etc. IM^{2}ODE can easily predict the atomic configurations with desired properties for three dimensional structure, interface and cluster, even complex defect in solid. Tests have been run on multiple systems and it has been proved that IM^{2}ODE is highly efficient and reliable, which can be applied widely.

1. Introduction

Traditionally discovering new materials is a long and costly process including a huge amount of trial and error in the progress of synthesizing and testing. Theoretical designing of materials has been a long standing dream of the scientists. With the development of supercomputers and first principle methods, one can correctly predict most of the properties of a material if the atomic configuration is known. However, the inverse of this approach, finding a material with unknown structure and desired properties, is still a great challenge in material design.

One way to do inverse design is by scanning databases of structures previously found and substituting elements in those structures, which is known as 'high-throughput' (HT) computational materials design, focusing on finding different composites of compounds [1–7]. Another way is to figure out the atomic configuration of a fixed chemical system with the desired properties, which is often achieved by combining an atomic structure searching with first principle calculations of target properties. These methods were first proposed by Franceschetti and Zunger, using simulated annealing algorithm to predict the atomic configuration of $Al_{0.25}Ga_{0.75}As$ alloy with the largest optical band gap [8]. Later, genetic algorithm [9,10] and particle swarm optimization [11,12] are proposed to design ordered alloy and meta stable crystal phase with target electronic-structure property. However, these methods take desired properties into account while neglecting the total energy and it is possible that the structures found by those methods may have rather high energy.

Atomic structure is the most fundamental properties of materials. In the past two decades, quite a few global optimization methods were developed to search the atomic structures [13–17]. Some global optimization packages, such as USPEX [18] and CALYPSO [19], were developed to predict new crystal structures with lowest enthalpy at given external conditions (e.g., pressure). The process of structure prediction involves exploring the energy surface which involves a huge number of energy minima. Highly efficient and robust global optimization methods are applied to solve this problem for sampling the energy surface and find global minima. There is something in common between the structure prediction and inverse design: both of them needs to scan the energy surface. The key difference is that structure prediction only needs to find a structure with the lowest energy, while inverse design needs to find a structure with desired properties.

Based on global optimization methods, we have developed a novel method for "inverse design", which is named as IM^{2}ODE (inverse design of Materials by Multi-Objective Differential Evolution). In this code package, Multi-Objective optimization methods are applied to predict structures with respect to both total energy and properties. By extending the inverse design problem from the single-objective domain to the multi-objective domain, we are able to predict metastable structures of desired properties with relatively low energy. Among the numerous global optimization algorithms, Multi-Objective Differential Evolution (MODE) has been widely used and achieved great successes [20–22]. MODE is

* Corresponding author.

http://dx.doi.org/10.1016/j.commatsci.2014.10.054
0927-0256/

Carbon 109 (2016) 246–252

Contents lists available at ScienceDirect

Carbon

journal homepage: www.elsevier.com/locate/carbon

Hybrid crystalline sp^2–sp^3 carbon as a high-efficiency solar cell absorber

Yue-Yu Zhang [a, b], Shiyou Chen [c], Hongjun Xiang [a, b], Xin-Gao Gong [a, b, *]

[a] Key Laboratory for Computational Physical Sciences (MOE), State Key Laboratory of Surface Physics, Department of Physics, Fudan University, Shanghai, 200433, China
[b] Collaborative Innovation Center of Advanced Microstructures, Nanjing, 210093, China
[c] Key Laboratory of Polar Materials and Devices (MOE), East China Normal University, Shanghai, 200241, China

ARTICLE INFO

Article history:
Received 17 May 2016
Received in revised form
2 August 2016
Accepted 7 August 2016
Available online 9 August 2016

ABSTRACT

Carbon is a versatile element that has allotropes with both sp^2 (graphene) and sp^3 (diamond) bonding. However, none of the allotropes can be used as light-absorber materials in solar cells due to either too large or too small band gap. Here, we propose a novel concept that enables a tunable band gap of carbon phases with sp^2 carbon atoms within a sp^3 carbon structure. The tunability is due to the quantum confinement effect. By embedding the sp^2 atoms within the sp^3 structure, we can design new carbon allotropes with ideal optical properties for optoelectronic applications. Five carbon allotropes incorporated this structural feature were identified by combining this new concept with our freshly developed multi-objective inverse band structure design approach. They all have proper band gaps for optical absorption, and the simulated photovoltaic efficiency of C_{10}-C is even higher than conventional absorber materials such as GaAs, which indicates that C_{10}-C with mixed sp^2–sp^3 hybridization may have potential application as light-absorber material in electronic and optoelectronic devices.

1. Introduction

Carbon is a versatile element, whose electronic states allow for sp^3, sp^2 and even sp hybridization. Hence, carbon can form many allotropes (graphite, diamond, fullerenes, nanotubes, etc.) with various micro-textures (more or less ordered), different dimensionalities (from 0 to 3D), and a rich variety of electronic structures (from metal to insulator) [1–4]. The exploration of new carbon allotropes has been the focus of numerous theoretical and experimental investigations because of their importance in both fundamental science and potential practical applications [5–11]. The two most stable phases of carbon, i.e., sp^3 hybridized diamond and sp^2 hybridized graphite (graphene), have a wide band gap (5.5 eV) and a zero gap, respectively. Moreover, all the recently predicted sp^3 hybridized carbon allotropes [9,12–15] have large band gaps. Although carbon is abundant, cheap, nontoxic, and similar to silicon in its bonding motif, which makes it competitive for many applications, none of the allotropes are suitable for certain optoelectronic applications such as photovoltaic (PV) solar cells, for which direct band gaps between 1.0 and 1.5 eV are optimal [16].

The sp^3 hybridization in diamond gives a large band gap ~5.5 eV while the sp^2 hybridization in graphene has a zero band gap. If one can mix the sp^2–sp^3 carbon allotropes in some form, the result may possess intermediate band gaps and provide an opportunity for "engineered" electronic and optical properties. Experiments show that by compressing different raw sp^2 carbons allotropes, hybrid sp^2–sp^3 phases can be formed [17–22]. Ab initio calculations predicted two metallic phases with sp^2 and sp^3 hybridization, T6 and T14 carbon [23]. Hybrid sp^2–sp^3 carbon allotropes were also proposed as possible structures of cold compressed graphite, unfortunately the resulting band gaps are still either too large or too small for the PV application [24]. However, those studies indicated that hybrid sp^2–sp^3 carbon allotropes may display drastically different electronic and optical properties.

If sp^2–sp^3 mixed hybridization in carbon materials can be engineered with tunable the band gaps in the range 1.0–1.5 eV, it becomes possible to design new carbon allotropes that may be ideal solar cell absorber materials, in contrast to all currently known carbon allotropes.

* Corresponding author. Key Laboratory for Computational Physical Sciences (MOE), State Key Laboratory of Surface Physics, Department of Physics, Fudan University, Shanghai, 200433, China.
E-mail address: xggong@fudan.edu.cn (X.-G. Gong).

http://dx.doi.org/10.1016/j.carbon.2016.08.015
0008-6223/

Origin of the type-II band offset between rutile and anatase titanium dioxide: Classical and quantum-mechanical interactions between O ions

Yue-Yu Zhang,[1,2] Li Lang,[1,2] Hui-Jun Gu,[1,2] Shiyou Chen,[3] Zhi-Pan Liu,[4] Hongjun Xiang,[1,2] and Xin-Gao Gong[1,2,*]

[1]*Key Laboratory for Computational Physical Sciences (MOE), State Key Laboratory of Surface Physics, Department of Physics, Fudan University, Shanghai 200433, China*

[2]*Collaborative Innovation Center of Advanced Microstructures, Nanjing 210093, China*

[3]*Key Laboratory of Polar Materials and Devices (MOE), East China Normal University, Shanghai 200241, China*

[4]*Key Laboratory of Computational Physical Science (MOE), Shanghai Key Laboratory of Molecular Catalysis and Innovative Materials, Department of Chemistry, Fudan University, Shanghai 200433, China*

(Received 14 February 2017; published 10 April 2017)

Titanium dioxide is one of the most promising semiconductors for photocatalytic splitting of water for hydrogen. The mixed rutile/anatase system shows even more favorable photocatalytic properties than the pristine ones. Band offset is a key factor that determines the photocatalytic activity of the mixed phase. However, the type of band alignment and the value of the band offset are still under debate both experimentally and theoretically. The difficulty of determining the band offset by commonly used core-level alignment calculation lies in the different symmetry and large lattice mismatch between the two phases. Here, we adopt our recently developed three-step method, which can overcome the lattice mismatch problem, to study the band offset with high accuracy. In the calculation, we used an intermediate phase TiO_2II to build superlattice models of rutile(101)//TiO_2II(001) and TiO_2II(100)//anatase(112) to determine the core-level alignment. Our studies show a type-II, staggered band alignment, with the valence band maximum (VBM) of rutile 0.80 eV above that of anatase, in agreement with recent experimental results. We further analyzed the electronic structure of the two phases, and found that the band offsets of the VBM originate from both the electrostatic interaction and electronic hybridization in rutile and anatase, which contribute 0.36 eV and 0.44 eV, respectively.

DOI: 10.1103/PhysRevB.95.155308

I. INTRODUCTION

Titanium dioxide (TiO_2) is widely used in solar cells, photocatalysts, and pigmentationx [1–6]. In the past several decades, a tremendous amount of experimental and theoretical research has studied its photoactivity since Fushijima and Honda [7] discovered the photoelectrochemical activity of TiO_2 anodes in 1971. Among the many polymorphs of TiO_2, rutile, anatase, and brookite are the most common. Rutile and anatase have wide band gaps of 3.03 and 3.20 eV, respectively, which lead to a low absorption efficiency in the solar spectrum [8]. It has been a longstanding puzzle why mixed-phase TiO_2 has better photocatalytic properties than either single-crystal rutile or anatase [9–14]. The reason for the increased reactivity may be attributable to several factors, including charge separation and interfacial charge transfer effects, which come down to the band offset problem.

The physical mechanism between the band offset of rutile and anatase is still unclear, even though large efforts have been made both experimentally and theoretically [15,16]. Through electrochemical impedance analysis, Kavan *et al.* [17] found that the conduction band of anatase is 0.2 eV above that of rutile (type-II rutile), which would cause the transfer of holes from rutile to anatase, as observed in other experiments [18,19]. However, recent x-ray photoelectron spectroscopy (XPS) measurements showed that the conduction band of anatase is 0.2 eV [20] or 0.6 $\sim$ 0.8 eV [21] below that of rutile (type-II anatase). Hence, the issue of the band offset between rutile and anatase is still under debate experimentally. A computational approach may clarify this debate, but it is difficult to obtain the band offset between rutile and anatase directly because it has not been possible to construct a heterostructure interface that preserves the bulk structures on both sides of the interface. Various attempts were made to calculate the band offset, such as the branch point energy (BPE) method, the passivated quantum dot (QD) method, electronic potential profiling (EPP) [22–24], the energetics of localized holes or electrons in biphase crystals [25], and quantum-mechanical/molecular-mechanical (QM/MM) method [20,26,27]. The BPE method calculates the band offset by sampling the bulk band structure. In QD calculations, large supercells of different phases are built to calculate the band offset by aligning the core-level energy. The EPP method calculates the band offset by measuring the electronic potential of a superlattice, containing over 1000 atoms built with two different phases of TiO_2 [24,28]. QM/MM calculates the band offset by a core-shell model. BPE only considers the bulk properties and discards the interfacial effects, while the other methods face the problem of constructing an interface between two different phases. The band offset between rutile and anatase measured or calculated are all listed in Table I. Up to now, neither the experimental nor the computational results agree with each other, as discussed in a recent article [16].

To definitely clarify the band offset between rutile and anatase, we have combined our newly developed three-step method [29] and the core-level alignment method with a special construction of interface. The core-level alignment method is believed to be a reliable method, which can predict the band offset with high precision [30]. However, this method cannot be directly applied to calculate the band alignment of rutile and anatase because of the difficulty in

*Corresponding author: xggong@fudan.edu.cn

CHIN. PHYS. LETT. Vol. 35, No. 3 (2018) 036104 **Express Letter**

Intrinsic Instability of the Hybrid Halide Perovskite Semiconductor $CH_3NH_3PbI_3$ *

Yue-Yu Zhang(张越宇)[1], Shiyou Chen(陈时友)[2**], Peng Xu(许朋)[1], Hongjun Xiang(向红军)[1], Xin-Gao Gong(龚新高)[1**], Aron Walsh[3], Su-Huai Wei(魏苏淮)[4]

[1]*Key Laboratory for Computational Physical Sciences (MOE), State Key Laboratory of Surface Physics, and Department of Physics, Fudan University, Shanghai 200433*

[2]*Key Laboratory of Polar Materials and Devices (MOE), East China Normal University, Shanghai 200241*

[3]*Center for Sustainable Chemical Technologies and Department of Chemistry, University of Bath, Bath BA2 7AY, UK*

[4]*Beijing Computational Science Research Center, Beijing 100094*

(Received 9 February 2018)

The organic-inorganic hybrid perovskite $CH_3NH_3PbI_3$ has attracted significant interest for its high performance in converting solar light into electrical power with an efficiency exceeding 20%. Unfortunately, chemical stability is one major challenge in the development of $CH_3NH_3PbI_3$ solar cells. It was commonly assumed that moisture or oxygen in the environment causes the poor stability of hybrid halide perovskites, however, here we show from the first-principles calculations that the room-temperature tetragonal phase of $CH_3NH_3PbI_3$ is thermodynamically unstable with respect to the phase separation into $CH_3NH_3I + PbI_2$, i.e., the disproportionation is exothermic, independent of the humidity or oxygen in the atmosphere. When the structure is distorted to the low-temperature orthorhombic phase, the energetic cost of separation increases, but remains small. Contributions from vibrational and configurational entropy at room temperature have been considered, but the instability of $CH_3NH_3PbI_3$ is unchanged. When I is replaced by Br or Cl, Pb by Sn, or the organic cation CH_3NH_3 by inorganic Cs, the perovskites become more stable and do not phase-separate spontaneously. Our study highlights that the poor chemical stability is intrinsic to $CH_3NH_3PbI_3$ and suggests that element-substitution may solve the chemical stability problem in hybrid halide perovskite solar cells.

PACS: 61.72.J−, 61.50.Ah, 71.20.Nr, 71.55.Gs DOI: 10.1088/0256-307X/35/3/036104

Inorganic-organic hybrid perovskite compounds ($CH_3NH_3PbX_3$, $X = $ I, Br and Cl) have been intensively studied as light-harvesting semiconductors in solar cells because of their strong optical absorption and high carrier mobility.[1−9] The power conversion efficiency (PCE) increases rapidly in the past three years, and now it is over 20%,[10,11] close to the record efficiency of the conventional silicon crystal,[12,13] CdTe[14] and Cu(In,Ga)Se_2[15] thin film solar cells which have been studied for several decades.

Despite the competitive photovoltaic efficiency, a major challenge is the poor material stability, which remains an obstacle in the development of commercially viable $CH_3NH_3PbI_3$ solar cells.[16−22] The degradation process of perovskite-structured $CH_3NH_3PbI_3$ can occur easily in humid environments, thus the device fabrication should be carried out with a humidity <1%, as suggested by Grätzel and coworkers.[2] However, the microscopic origin and detailed process of the degradation is still unclear. The experiments of Niu *et al.* showed that moisture, oxygen and UV radiation play a role in the degradation progress of perovskite $CH_3NH_3PbI_3$.[23] On the other hand, Schoonman proposed that the Pb-I components of the perovskite structure may exhibit photodecomposition similar to that of the binary halides.[24] This process is easy to understand, as the upper valence band is formed by the antibonding states of the Pb 6*s*–I 5*p* hybridization,[25,26] which increases the dispersion of the valence bands (thus small hole effective masses[27]) but also weakens the Pb-I bonds.

Although the poor stability of $CH_3NH_3PbI_3$ can be understood from different perspectives, it is generally assumed that $CH_3NH_3PbI_3$ is a stable compound with respect to the phase separation, i.e., it will not disproportionate spontaneously.[28] If this assumption is true, the degradation of $CH_3NH_3PbI_3$ solar cells can be suppressed if the compound is protected from the moisture, oxygen and light-illumination. In contrast, we demonstrate that $CH_3NH_3PbI_3$ in the room-temperature tetragonal structure is thermodynamically unstable, and phase separation into the

The work at Fudan University was supported by the Special Funds for Major State Basic Research, National Natural Science Foundation of China (NSFC), and Project of Shanghai Municipality (16520721600). S.C. was supported by NSFC under Grant No 91233121, Shanghai Rising-Star Program (14QA1401500) and CC of ECNU. The work at Bath was supported by the Royal Society, the ERC and EPSRC under Grant Nos EP/M009580/1 and EP/K016288/1. S.H.W. was supported by the National Key Research and Development Program of China under Grant No 2016YFB0700700, and the National Natural Science Foundation of China under Grant Nos 51672023, 11634003 and U1530401.

**Corresponding author. Email: chensy@ee.ecnu.edu.cn; xggong@fudan.edu.cn

The Journal of Chemical Physics ARTICLE scitation.org/journal/jcp

Improving collective variables: The case of crystallization

Cite as: J. Chem. Phys. 150, 094509 (2019); doi: 10.1063/1.5081040
Submitted: 13 November 2018 • Accepted: 8 February 2019 •
Published Online: 7 March 2019

Yue-Yu Zhang,[1,2] Haiyang Niu,[1,2] GiovanniMaria Piccini,[1,2] Dan Mendels,[1,2] and Michele Parrinello[1,2,a)]

AFFILIATIONS

[1]Department of Chemistry and Applied Biosciences, ETH Zurich, c/o USI Campus, Via Giuseppe Buffi 13, CH-6900 Lugano, Ticino, Switzerland

[2]Institute of Computational Science, Università della Svizzera Italiana (USI), Via Giuseppe Buffi 13, CH-6900 Lugano, Ticino, Switzerland

[a)]E-mail: parrinello@phys.chem.ethz.ch

ABSTRACT

Several enhanced sampling methods, such as umbrella sampling or metadynamics, rely on the identification of an appropriate set of collective variables. Recently two methods have been proposed to alleviate the task of determining efficient collective variables. One is based on linear discriminant analysis; the other is based on a variational approach to conformational dynamics and uses time-lagged independent component analysis. In this paper, we compare the performance of these two approaches in the study of the homogeneous crystallization of two simple metals. We focus on Na and Al and search for the most efficient collective variables that can be expressed as a linear combination of X-ray diffraction peak intensities. We find that the performances of the two methods are very similar. Wherever the different metastable states are well-separated, the method based on linear discriminant analysis, based on its harmonic version, is to be preferred because simpler to implement and less computationally demanding. The variational approach, however, has the potential to discover the existence of different metastable states.

I. INTRODUCTION

Many chemical and physical phenomena are characterized by the occurrence of long lived metastable states. Under these circumstances, accurate sampling becomes computationally expensive or even prohibitive. In order to overcome this problem, many methods have been suggested.[1] A large fraction of these methods depends on the definition of collective variables (CVs). Typical examples are umbrella sampling,[2–5] metadynamics,[6–9] and variationally enhanced sampling.[10] The efficiency of these simulations depends very much on the quality of the CV, and hence, the finding and improving of CVs is the object of intense investigations.[11]

In our group, two methods have recently been developed, harmonic linear discriminant analysis (HLDA)[12] and variational approach to conformational dynamics (VAC).[13] In HLDA, one constructs low dimensional CVs from the local fluctuations in the different metastable states. In contrast, in the VAC approach, one starts with a biased simulation with non-optimal CVs and attempts to improve this initial guess using a variational principle approach that is based on the time-lagged independent component analysis (TICA).

In this work, we compare the performance of HLDA-generated CVs with those obtained using VAC. We focus on a typical application area of enhanced sampling methods, namely, homogeneous crystallization. In particular, we shall present results on two systems, Na and Al, already studied elsewhere.[4,5,9,14]

It has recently been shown[15] that the X-ray diffraction (XRD) intensities can be useful CVs. However, sometimes a single peak is not sufficient. Thus we shall search with HLDA and VAC for the best linear combinations of the diffraction peak intensities. We are not implying here that XRD intensities are necessarily the best possible CVs to study nucleation. However, they have been successfully used and provided a good example on how to improve from reasonable CVs, which is the situation commonly encountered in the practice.

THE JOURNAL OF PHYSICAL CHEMISTRY C

Article

pubs.acs.org/JPCC

Predicting New TiO_2 Phases with Low Band Gaps by a Multiobjective Global Optimization Approach

Hou-Zun Chen,† Yue-Yu Zhang,† Xingao Gong,* and Hongjun Xiang*

Key Laboratory of Computational Physical Sciences (Ministry of Education), State Key Laboratory of Surface Physics, and Department of Physics, Fudan University, Shanghai 200433, P. R. China

Supporting Information

ABSTRACT: TiO_2 has been extensively studied due to the possible application in solar cells and photoelectrochemical (PEC) water-splitting. However, the energy conversion efficiency is rather low because of the large band gaps (larger than 3.0 eV) of rutile and anatase TiO_2. Here we introduce the multiobjective differential evolution (MODE) method as a novel global optimization algorithm to predict new polymorphs of bulk TiO_2 with better optical properties than rutile and anatase TiO_2. The band gaps of the new PI (*Pnma*) and CI (C2) phases are found to be 1.95 and 2.64 eV. The calculation of formation energy, phonon dispersions, and thermal stability shows that the two novel phases are dynamically and thermally stable. These new TiO_2 polymorphs with better electronic and optical properties may pave a new way for high-efficiency solar energy conversion.

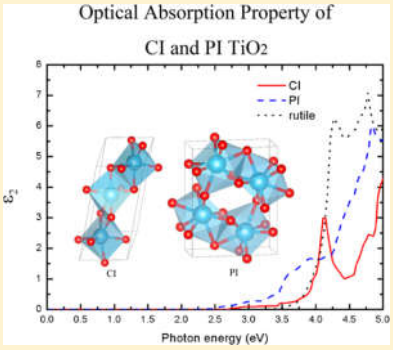

INTRODUCTION

Titanium dioxide (TiO_2) is a wide-gap semiconductor that can be widely used in applications from solar cells to photocatalyst and pigmentation.[1,2] In the past several decades, the tremendous amount of experimental and theoretical research has been performed in the field of semiconductor photocatalyst since Fushijima and Honda discovered the photoelectrochemistry (PEC) effect on anode TiO_2 in 1971.[3] TiO_2 was also used as the common photocathode in dye-sensitized solar cells.[4] For both water splitting and dye-sensitized solar cell applications, the optimal band gap for the oxide should be around 2.0 eV. However, the large band gap of TiO_2 (3.2 eV for the anatase phase and 3.0 eV for the rutile phase) leads to low absorption efficiency in the solar emission spectra. Different methods have been applied to narrow the gap of TiO_2 to make it suitable for sunlight absorption.[5−7] The most widely used approach is doping, but doping-induced charge carrier trapping and recombination sites could reduce the photochemical activity of TiO_2.[8] Therefore, a dopant-free TiO_2 phase with a suitable band gap is highly desirable.

In this article, we predict new metastable TiO_2 phases with low band gaps for the use as solar cells. To achieve this target, we propose a general multiobjective global optimization algorithm [i.e., multiobjective differential evolution (MODE)] for inverse design of materials. In this novel method, more than one objective function can be optimized simultaneously, for example, total energy, band gap, hardness, etc. Here, we are trying to search a TiO_2 phase that has better optical properties than rutile phase and is also relatively stable. This is equivalent to a global optimization problem of a biobjective function, i.e., total energy and band gap. By combining the MODE method with density functional calculations, we find numerous new metastable structures of TiO_2 with the band gap around 2.3 eV. In particular, the *Pnma* and C2 phases have band gaps of 1.95 and 2.64 eV, respectively. They are only 0.15 eV/atom and 0.11 eV/atom less stable than the rutile TiO_2, respectively.

METHODS

2.1. Multiobjective Differential Evolution (MODE) for Inverse Design. In the past two decades, great efforts have been made in crystal structure prediction, and various algorithms have been developed,[9−14] most of which only search for structures with the lowest total energy. In application, special properties such as light absorption, hardness, etc., are of great concern. Some methods take those properties into account while neglecting the total energy,[15,16] and it is possible that the structures found by those methods may have rather high energy.

Here, we developed a novel method for inverse design through applying multiobjective optimization methods to predict structures with respect to both total energy and properties, thus extending the crystal structure prediction problem from the single-objective domain to the multiobjective domain. For multiobjective problems, there is a set of optimal functions, so a Pareto front will be found, which is formed by several alternative optimal solutions in the search space. However, in traditional mathematical programming techniques,[17] the objectives are weighted and summed into a single goal, which do not consider all the objectives simultaneously and most of which find only a single optimal solution instead of

Received: November 20, 2013
Revised: January 9, 2014
Published: January 14, 2014

   dx.doi.org/10.1021/jp411437f | J. Phys. Chem. C 2014, 118, 2333−2337

shown in Figure 4a,b. It is obvious that the CI has a direct band gap with $E_g \approx 2.64$ eV, while the PI is an indirect gap material

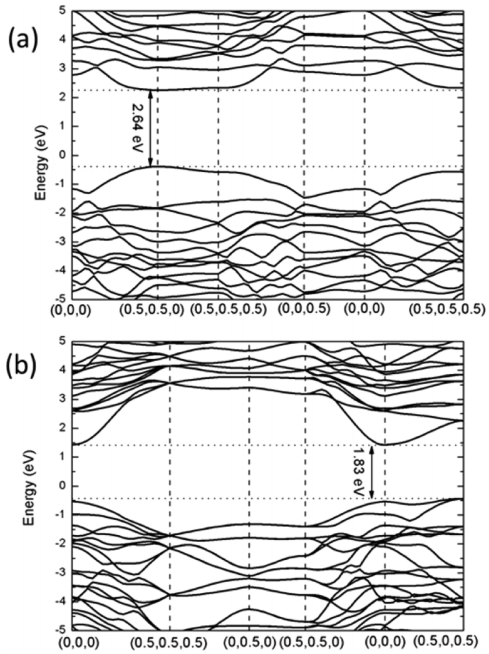

Figure 4. (a,b) HSE06 band structure of CI and PI. Both the VBM and CBM are denoted by dotted lines. The *k* points are shown by the fractional coordinates in the terms of the reciprocal lattice of the unit-cell. As we can see from the figure, the direct band gap (2.64 eV) of CI locates at (0.5, 0.5, 0). The VBM and CBM of PI appeared at (0.5, 0, 0.5) and (0, 0, 0), respectively. The direct gap is 1.95 eV, which is located at the gamma point.

with a direct gap of 1.95 eV and an indirect gap of 1.83 eV. We note that the structure of OII (one of the known polymorphs of TiO_2) with the same space group (*Pnma*) is similar to that of PI. The only structural difference (see Figure 3b,c) is that each Ti atom is 8-fold coordinated in PI but 9-fold coordinated in OII. The HSE06 band gap of OII is 3.01 eV, which is much larger than that (1.95 eV) of PI.

3.2.3. Optical Property. It is well-known that the imaginary part of the dielectric tensor $\varepsilon_2(\omega)$ determines the absorption ability of a material. Here we also adopt the HSE06 functional to compute $\varepsilon_2(\omega)$ accurately. Figure 5 shows the $\varepsilon_2(\omega)$ curves of the two new polymorphs with black and pink lines, respectively. For comparison, the corresponding results of rutile, anatase, brookite, OII, pyrite, and fluorite TiO_2 are also shown in the same figure. As we can see in Figure 5, the curves of CI and PI both rise before rutile and anatase, which indicate that PI and CI are better light absorbers than rutile and anatase. The curve of PI rises at about 2.5 eV; therefore, the absorption of PI can be extended to the visible region of the solar spectrum. The light absorption ability of PI is close to that of fluorite, which was also proposed to be a potential light absorber.[31] However, fluorite is not stable in standard ambient conditions because of the presence of imaginary frequencies in the phonon spectra, while PI and CI are dynamically stable. Furthermore, the PI and CI phases are found to be more stable than fluorite TiO_2 by −0.04 and −0.08 eV/atom, respectively.

As can be seen from Figure 5, CI TiO_2 starts to absorb light at an energy of the direct band gap (2.64 eV). This is because

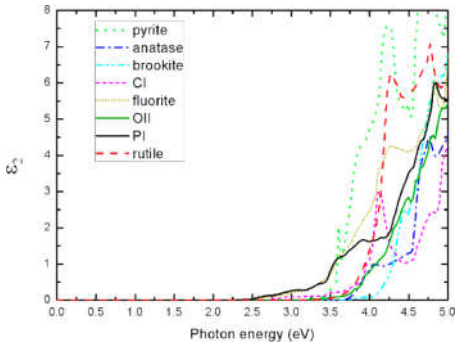

Figure 5. Imaginary part of dielectric functions of the two new TiO_2 polymorphs from the HSE06 calculations. For comparison, the imaginary part of dielectric functions of anatase, brookite, rutile, pyrite, fluorite, and OII from HSE06 is also shown.

all dipole transitions (including the direct band gap transition) in any system with a C_2 point group is allowed. However, PI TiO_2 starts to absorb light at 2.5 eV, which is larger than the electronic direct band gap (1.95 eV). We find that both VBM and CBM states at Γ have odd parity symmetry; thus, the direct band gap dipole transition is forbidden.

CONCLUSIONS

In summary, we developed a novel global optimization algorithm (i.e., multiobjective differential evolution (MODE)) to predict new material that possesses several desirable properties (for example, a low energy and a given band gap) simultaneously. By combining this method with first-principle calculations, we predict two new low band gap metastable TiO_2 phases (PI and CI) for solar energy applications. These two phases are found to have a better light absorption ability than other well-known TiO_2 polymorphs, and they are only slightly less stable (about 0.1 eV/atom) than rutile TiO_2. These news TiO_2 polymorphs are found to be both thermally and dynamically stable, which may be used in solar energy systems to improve the energy conversion efficiency. Furthermore, our MODE approach for inverse material design will pave a new way for predicting and designing other functional materials.

ASSOCIATED CONTENT

Supporting Information

Phonon dispersions and potential energies. This material is available free of charge via the Internet at http://pubs.acs.org.

AUTHOR INFORMATION

Corresponding Authors

*(X.G.) E-mail: xggong@fudan.edu.cn.
*(H.X.) E-mail: hxiang@fudan.edu.cn.

Author Contributions

†H.-Z.C. and Y.-Y.Z. contributed equally to this work.

Notes

The authors declare no competing financial interest.

ACKNOWLEDGMENTS

The authors thank Yang Zhou for completing part of the Inverse-Design of Materials by Multi-Objective Differential Evolution (IM^{2}ODE) package of structure searching and Hai-Yuan Cao for useful discussions. Work was supported by NSFC, the Special Funds for Major State Basic Research,

analytical chemistry

Article

pubs.acs.org/ac

Mesoporous Fe_2O_3–CdS Heterostructures for Real-Time Photoelectrochemical Dynamic Probing of Cu^{2+}

Jing Tang,[†,∥] Jun Li,[†,∥] Yueyu Zhang,[‡,∥] Biao Kong,[†] Yiliguma,[†] Yang Wang,[†] Yingzhou Quan,[†] Hao Cheng,[†] Abdullah M. Al-Enizi,[§] Xingao Gong,[‡] and Gengfeng Zheng*[,†]

[†]Laboratory of Advanced Materials, Department of Chemistry, Collaborative Innovation Center of Chemistry for Energy Materials, Fudan University, Shanghai 200433, China

[‡]Center for Key Laboratory of Computational Physical Sciences, Ministry of Education, State Key Laboratory of Surface Physics, and Department of Physics, Fudan University, Shanghai 200433, China

[§]Department of Chemistry-College of Science, King Saud University, Riyadh 11451, Saudi Arabia

Supporting Information

ABSTRACT: A three-dimensional (3D) mesoporous Fe_2O_3–CdS nanopyramid heterostructure is developed for solar-driven, real-time, and selective photoelectrochemical sensing of Cu^{2+} in the living cells. Fabrication of the mesoporous Fe_2O_3 nanopyramids is realized by an interfacial aligned growth and self-assembly process, based on the van der drift model and subsequent selective in situ growth of CdS nanocrystals. The as-prepared mesoporous Fe_2O_3–CdS heterostructures achieve significant enhancement (~3-fold) in the photocurrent density compared to pristine mesoporous Fe_2O_3, which is attributed to the unique mesoporous heterostructures with multiple features including excellent flexibility, high surface area (~87 m^2/g), and large pore size (~20 nm), enabling the PEC performance enhancement by facilitating ion transport and providing more active electrochemical reaction sites. In addition, the introduction of Cu^{2+} enables the activation of quenching the charge transfer efficiency, thus leading to sensitive photoelectrochemical recording of Cu^{2+} level in buffer and cellular environments. Furthermore, real-time monitoring (~0.5 nM) of Cu^{2+} released from apoptotic HeLa cell is performed using the as-prepared 3D mesoporous Fe_2O_3–CdS sensor, suggesting the capability of studying the nanomaterial–cell interfaces and illuminating the role of Cu^{2+} as trace element.

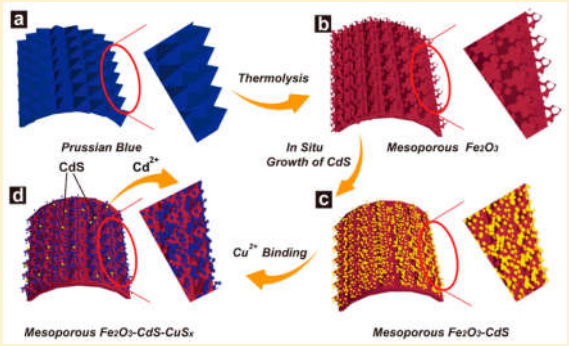

Fundamental cellular functions and medical research have elucidated the function mechanism of many physiological trace elements, which have the potential to greatly improve disease diagnosis.[1−5] Among all the trace elements, copper is an important metal that is essential for most forms of life and the third most abundant transition metal in humans,[6−8] which serves as a structural and catalytic cofactor for many proteins and enzymes such as cytochrome *c* oxidase and copper–zinc superoxide dismutase.[9] Understanding how copper contributes to healthy and disease states requires advanced methods for real-time dynamic probing copper in the living cells rather than in ionic or molecular models.[10] Several methods have been demonstrated to probe Cu^{2+} in biological environments.[11,12] Nonetheless, the ultralow concentrations and complex forms of Cu^{2+} in living cells pose a challenging barrier to monitor the real-time dynamic production and concentration of Cu^{2+} in physiological conditions.[13]

Semiconductor-based photoelectrochemical (PEC) biomolecule detection is a recently developed sensing approach that represents several attractive features.[14−20] First, light and electricity inducers effectively eliminate the signal excitation and detection from the background noise.[21] Second, the semiconductor nanostructure PEC conversion enables a combination of low intensity light source (such as sunlight) and low electric field for generation of reactive charge carriers and photocurrent, which facilitate the targeted electrochemical reactions without other possible interfering side reactions.[22] Third, compared to conventional electrochemical detections progressing on the electrode surfaces, the PEC method can realize the evolution of oxygen or other reactive oxidative species in the interiors of bulky biomolecules, offering charge relay and efficient signal transducing.[23] Among the semiconductor materials for the PEC conversion, α-Fe_2O_3 has been demonstrated as one of the most attractive candidates for PEC probing, due to its suitable band gap size (1.9–2.2 eV), photo- and electrochemical stability, nontoxicity, low cost, and earth abundancy.[24−26] Despite these seemingly favorable characteristics, several factors have limited the α-Fe_2O_3 photoactivity performance,[24] including a short hole diffusion length (2–4

Received: March 3, 2015
Accepted: June 12, 2015
Published: June 12, 2015

DOI: 10.1021/acs.analchem.5b00844
Anal. Chem. 2015, 87, 6703–6708

assay leads to significant photocurrent change, confirming our proposed detection mechanism. As demonstrated above, our approach for Cu^{2+} detection shows high selectivity, suggesting the present PEC sensor can potentially be applied for detecting Cu^{2+} in living biosystems.[37−39]

The capability of the mesoporous Fe_2O_3−CdS PEC sensors for recording of Cu^{2+} release from living cells is further investigated (Figure 5a). In the process, Hela cells were directly

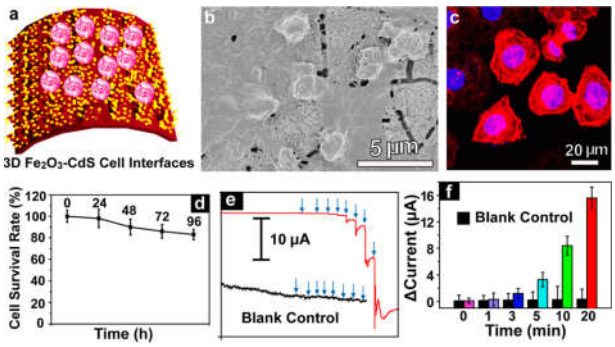

Figure 5. 3D mesoporous nano-cell interfaces for real-time photoelectrochemical dynamic probing of Cu^{2+}. (a) Schematic representation of living cells cultured on Fe_2O_3−CdS. (b) SEM images of fixed Hela cells on Fe_2O_3−CdS films. (c) Fluorescence images of Hela cells cultured on the Fe_2O_3−CdS. The cells were stained with phalloidin-tetramethylrhodamine B isothiocyanate for F-actin (red), 4′,6-diamidino-2-phenylindole dihydrochloride (DAPI) for nuclei (blue). (d) Percentage of viable HeLa cells cultured on the Fe_2O_3−CdS. (e, f) Real-time detection of Cu^{2+} by the Fe_2O_3−CdS PEC sensor, when trypsin was added at different time to the cell culture. A similar PEC sensor but without cell culture was used as the blank control.

cultured on top of the mesoporous Fe_2O_3−CdS arrays to reach the growth confluence, preserving well-conditioned morphologies and tight contact to the mesoporous Fe_2O_3−CdS interfaces judged by SEM images (Figure 5b). Then, fluorescence imaging was employed to observe the living Hela cells, in which F-actins and nuclei were labeled by phalloidin-tetramethylrhodamine B isothiocyanate (red color) and 4′,6-diamidino-2-phenylindole dihydrochloride (DAPI, blue color), respectively (Figure 5c). The Hela cells show normal morphologies, active cell functions and proliferation with its viability retained at >90% and >85% over 24, 48, 72, and 96 h growth on the nanopyramids, respectively, indicating low cytotoxicity of the sensor platform for cell culture (Figure 5d). This phenomenon implies the potential application of 3D mesoporous Fe_2O_3−CdS nanopyramids in real-time and in situ monitoring of the complex Cu^{2+} released from biosystems.

The mesoporous Fe_2O_3−CdS nanopyramid biosensor is further explored for the PEC probing of Cu^{2+} released from living cells. During the digestion and apoptosis processes of cells generated by trypsin, the Cu^{2+} ions (in both free and complex forms) are released,[47] which can be evaluated the 3D mesoporous Fe_2O_3−CdS PEC sensor. The real-time monitoring shows that discrete photocurrent increases are repeated observed upon the corresponding addition of trypsin into the Hela cell culture (Figure 5e,f), indicating the excellent capability of direct culturing and PEC detection of the important cellular molecules by the nanopyramids. It should also be noted that both free and complex Cu^{2+} ions are released from the cells. In order to accurately determine the exact Cu^{2+} concentrations in cells, more detailed calibrations of different complex forms of Cu^{2+} ions are required with standard samples such as [Cu−Zn] superoxide dismutase,[47] in addition to free Cu^{2+} ions. Furthermore, it is possible that some organic molecule interferences can act as the hole scavengers and affect the PEC signal. However, the charge transfer sensitization between CdS (or CuS_x) and Fe_2O_3 has a much more significant effect on the photocurrent density and the sensing signal. Therefore, our system can still present good selectivity in biological systems. In contrast, Fe_2O_3−CdS without the cells do not show signals, indicating the selectivity of our PEC sensors (Figure 5e,f). The robust sensing performance and long-term function stability of the 3D mesoporous Fe_2O_3−CdS PEC sensor is attributed to the stable structures and optoelectronic performances of CdS sensitizer and 3D mesoporous Fe_2O_3, as well as their strong chemical binding. These results further suggest that the present 3D mesoporous Fe_2O_3−CdS can be further used to detect the Cu^{2+} in various biosystems.

CONCLUSIONS

In summary, a sensing platform using 3D mesoporous Fe_2O_3−CdS nanopyramid heterostructure for solar-driven, real-time, and selective photoelectrochemical sensing of Cu^{2+} is developed. Compared to conventional sensing approaches, the 3D mesoporous Fe_2O_3−CdS nanopyramid sensors display several significant advantages, excellent biocompatibility, including effectively reduction of background interference, simplicity, rapid response, excellent flexibility, and low cost for practical bioapplications. This promising sensing platform enables rapid and accurate diagnosis for Cu^{2+} with a low detection limit (~0.5 nM). Furthermore, the fabrication and investigation of 3D mesoporous nanopyramids provide a new paradigm for fabrication of unconventional solar-driven mesoporous heterostructures and further suggest a new strategy for designing a low-cost and sensitive photoelectrochemical dynamic sensing interface toward living cells.

ASSOCIATED CONTENT

Supporting Information

Supporting figures S1−S13 and Table S1. The Supporting Information is available free of charge on the ACS Publications website at DOI: 10.1021/acs.analchem.5b00844.

AUTHOR INFORMATION

Corresponding Author

*E-mail: gfzheng@fudan.edu.cn (G.Z.).

Author Contributions

‖These authors contributed equally (J.T., J.L. and Y.Z.).

Notes

The authors declare no competing financial interest.

ACKNOWLEDGMENTS

We thank the following funding agencies for supporting this work: the National Key Basic Research Program of China (2013CB934104), the Natural Science Foundation of China (21322311, 21473038), the Science and Technology Commission of Shanghai Municipality (14JC1490500), the Program for Professor of Special Appointment (Eastern Scholar) at Shanghai Institutions of Higher Learning, and the Collaborative Innovation Center of Chemistry for Energy Materials (2011-iChem). J.L. and Y.Q. acknowledge the support of Hui-Chun Chin and Tsung-Dao Lee Chinese Undergraduate Research Endowment, Wang-Dao Undergraduate Research Funding, and

DOI: 10.1021/acs.analchem.5b00844
Anal. Chem. 2015, 87, 6703−6708

Nanoscale

PAPER

View Article Online
View Journal | View Issue

Cite this: *Nanoscale*, 2016, **8**, 5786

Three-dimensional WS_2 nanosheet networks for H_2O_2 produced for cell signaling†

Jing Tang,‡[a] Yingzhou Quan,‡[a] Yueyu Zhang,‡[b] Min Jiang,[c] Abdullah M. Al-Enizi,[d] Biao Kong,[a] Tiance An,[a] Wenshuo Wang,[e] Limin Xia,[e] Xingao Gong[b] and Gengfeng Zheng*[a]

Received 28th December 2015,
Accepted 8th February 2016

DOI: 10.1039/c5nr09236a

www.rsc.org/nanoscale

Hydrogen peroxide (H_2O_2) is an important molecular messenger for cellular signal transduction. The capability of direct probing of H_2O_2 in complex biological systems can offer potential for elucidating its manifold roles in living systems. Here we report the fabrication of three-dimensional (3D) WS_2 nanosheet networks with flower-like morphologies on a variety of conducting substrates. The semiconducting WS_2 nanosheets with largely exposed edge sites on flexible carbon fibers enable abundant catalytically active sites, excellent charge transfer, and high permeability to chemicals and biomaterials. Thus, the 3D WS_2-based nano-bio-interface exhibits a wide detection range, high sensitivity and rapid response time for H_2O_2, and is capable of visualizing endogenous H_2O_2 produced in living RAW 264.7 macrophage cells and neurons. First-principles calculations further demonstrate that the enhanced sensitivity of probing H_2O_2 is attributed to the efficient and spontaneous H_2O_2 adsorption on WS_2 nanosheet edge sites. The combined features of 3D WS_2 nanosheet networks suggest attractive new opportunities for exploring the physiological roles of reactive oxygen species like H_2O_2 in living systems.

1. Introduction

The three-dimensional (3D) nano-bio-interface has been attracting substantial research interest in chemistry, nanotechnology and life sciences in recent years.[1] Understanding the interplay of materials and energy at biological interfaces has inspired the rational design of 3D nano-bio-interfaces, which are endowed with advantages and capabilities in developing advanced biological science and technology.[1] Transition metal dichalcogenides (TMDs) are a group of unique 2D materials, owing to their intriguing layer-dependent electronic and optical properties.[2–5] Recent research studies have revealed the possibilities of nano-bio-interface based on TMDs with different morphologies for drug delivery,[6] sensing,[7,8] photothermal materials,[9] electroluminescence[10] and electrocatalysis.[11]

Among many reactive oxygen species (ROS), hydrogen peroxide (H_2O_2) is an important signal messenger molecule that triggers reversible post-translational modifications of downstream targets, such as phosphatases, ion channels, transcription factors and kinases.[12,13] It has also been realized that H_2O_2 plays essential functions in healthy physiological signaling pathways.[14] The capability of fast and sensitive H_2O_2 measurement especially in cellular environments and functions represents attractive advantages for understanding how cells produce, partition and funnel H_2O_2 into specific signaling pathways.[15,16] The use of ultrasmall MoS_2 platelets has recently been reported on the electrochemical detection of hydrogen peroxide (H_2O_2) secreted by living cells.[8] However, the development of the TMD-based nano-bio-interface with sensitive signal monitoring and probing of living cells is still at a very early stage, in which one of the significant challenges is to probe living cells grown on 3D structures that mimic real environments inside tissues. Solving this challenge requires the development of new probing platforms with high interaction interfaces, abundant active sites and easy accessibility, as well as sensitive and selective means for identifying the biosignals derived from cellular activities.[1]

In this work, we demonstrate the fabrication of a 3D flower-like tungsten sulfide (WS_2) nanosheet network with exposed edge sites grown on a large variety of substrates *via* a chemical

[a]*Laboratory of Advanced Materials, Department of Chemistry, Collaborative Innovation Center of Chemistry for Energy Materials, Fudan University, Shanghai 200433, China. E-mail: gfzheng@fudan.edu.cn*
[b]*Key Laboratory of Computational Physical Sciences, Ministry of Education, State Key Laboratory of Surface Physics, and Department of Physics, Fudan University, Shanghai 200433, China*
[c]*Institute of Brain Science and State Key Laboratory of Medical Neurobiology, Fudan University, Shanghai 200032, China*
[d]*Department of Chemistry, College of Science, King Saud University, Riyadh 11451, Saudi Arabia*
[e]*Department of Cardiovascular Surgery, Zhongshan Hospital, Fudan University, Shanghai 200032, China*
†Electronic supplementary information (ESI) available: Additional figures. See DOI: 10.1039/c5nr09236a
‡These authors contributed equally to this work.

ADVANCED MATERIALS
www.advmat.de

Materials Views
www.MaterialsViews.com

Achieving High Aqueous Energy Storage via Hydrogen-Generation Passivation

Yuhang Wang, Xiaoqi Cui, Yueyu Zhang, Lijuan Zhang, Xingao Gong, and Gengfeng Zheng**

Aqueous rechargeable lithium-ion batteries (ARLIBs) represent an extremely attractive candidate for next-generation energy-storage devices, attributed to their excellent theoretical power density, high ionic conductivity, nonflammability, and low cost.[1–3] Nonetheless, compared to their nonaqueous counterparts, the development of ARLIBs has been critically limited by their much narrower electrochemical potential windows (typically <1.8 V) and lower energy densities,[4,5] which are predominantly restrained by ubiquitous side reactions in aqueous solutions, i.e., electrochemical water splitting.[6] Although the sluggish oxygen evolution usually requires a large overpotential, the hydrogen-evolution reaction (HER) can easily take place when the applied potential increases, and thereby serves as a critical constraining factor for the battery voltage working window as well as the output Coulombic efficiency.[2,6] Although using alkaline electrolytes can shift the water reduction potential and allow for the functionality of anode materials,[1,7] the water oxidation potential also shifts downward, and thus the existence of water splitting with a thermodynamic potential of 1.23 V still results in a significant loss of Coulombic efficiency.[7] It was recently reported that using highly concentrated (molality > 20 m) organic Li^+ salt-based aqueous electrolytes can expand the voltage window.[8] However, such high salt concentrations inevitably lead to a much slower reaction kinetics of ARLIBs, and thereby a limited high-power feature.

The rational design of anode materials, in which the water reduction also takes place, may suggest a new avenue for ARLIB discovery with enhanced voltage window and power density. Our design was inspired by the recent research hotspots of developing new hydrogen-evolution catalysts that can reduce the overpotentials of hydrogen formation.[9–11] The opposite strategy instead, aiming to create a large HER overpotential for inhibiting water reduction and subsequently enhancing both the battery output potential and Coulombic efficiency in aqueous solutions, has never been demonstrated. Moreover, an electrode surface passivated with hydrogen evolution may further enable high current densities during battery cycling, leading to both an ultrahigh power density and an excellent energy density.

In this regard, electrochemically active materials with strong affinity to Li^+ ions but passivated HER activity of HER are of our highest interest. Particularly, polyimides (PIs) are a group of synthetic molecules with reversible redox capability, and have recently been reported as lithium- or sodium-ion-battery anode materials,[12–17] in which the intrinsic insulating behavior of PIs is resolved by the combination with conductive carbon materials.[12–15] Nonetheless, due to the lack of sufficient surface engineering for HER passivation and charge transport, the voltage output, and the power density of these electrodes are still far from optimum. We first carried out density functional theory (DFT) calculations to investigate the molecular structures of PIs, using two simple examples, poly(naphthalene four formyl ethylenediamine) (PNFE) and poly(benzene four formyl ethylenediamine) (PBFE). The most active sites for hydrogen atom adsorption in the PI structures are oxygen atoms, which possess the minimum value of energy barriers for binding an H atom (Table S1 in the Supporting Information). In an electrolyte without Li^+ ions, the activation barrier of the simulated reaction pathway of H_2 formation is 2.11 eV for PNFE (**Figure 1**a) and 1.94 eV for PBFE (Figure S1 in the Supporting Information), indicating an intrinsic sluggish response to HER. This high activation energy for H atom adsorption is general for different PI structures (Table S1 in the Supporting Information). In addition, during the battery charging process in a Li^+-containing electrolyte, half of the active sites (O atoms) for both Tafel ($2H_{adsorption} \rightarrow H_2$) and Heyrovsky ($H_{adsorption} + H_2O + e^- \rightarrow H_2 + OH^-$) are occupied by Li^+ ions (Figure 1b), leading to a higher energy barrier and more sluggish kinetics for H_2 formation. Subsequently, a larger potential window and much higher energy densities are expected.

Thus, based on our hydrogen-evolution passivation strategy and the aforementioned theoretical analysis, we have reported a polyimide (i.e., PNFE) nanosheet array structure uniformly grown on freestanding carbon nanotube (CNT) networks, for its passivated HER activities and electrochemical energy-storage performance as ARLIB anodes (Figure 1c). PNFE was grown in situ on and was fully covered over the underlying freestanding CNT networks, which serve as current collectors with a negligible contribution to capacity and Coulombic efficiency (Figure S2 in the Supporting Information), and afford a substantially passivated HER activity as well as capability for Li^+ storage. As a proof-of-concept, the PNFE nanosheets supported by freestanding CNT networks (designated as PNFE/CNT) display an extremely

Y. Wang, X. Cui, Dr. L. Zhang, Prof. G. Zheng
Laboratory of Advanced Materials
Department of Chemistry
Collaborative Innovation Center of Chemistry for Energy Materials
Fudan University
Shanghai 200433, China
E-mail: gfzheng@fudan.edu.cn
Y. Zhang, Prof. X. Gong
Department of Physics
Fudan University
Shanghai 200433, China
E-mail: xggong@fudan.edu.cn

DOI: 10.1002/adma.201602583

mass of PNFE and $LiMn_2O_4$. After 1000 cycles, the discharge capacity is retained at 45.1 mA h g^{-1} with a capacity retention of 65.5% (Figure 4b). The Coulombic efficiencies in majority of our 1000 cycles were ranging between 97% and 99%, except for the last 50 cycles (i.e., cycle 950–1000) the efficiency was ≈96%. The slight fading of Coulombic efficiency during the last 50 cycles is attributed to the electrochemical energy-storage process and capacity decay induced by long-term operation, similar to the recent literature,[8] instead of the hydrogen production due to water splitting. The open circuit voltage (OCV) of a fully charged PNFE//$LiMn_2O_4$ can be retained at ≈1.52 V after a standing time of 10 h (Figure S11 in the Supporting Information). A similar phenomenon was also reported previously in a polyimide//$LiMn_2O_4$ system with a much narrower voltage window,[16] indicating that the OCV decay is ascribed to its capacitive mechanism of energy storage, instead of water splitting. The discharging rate measurement was then performed at the current rate ranging from 2 to 100 C (Figure 4c). The discharge capacity at 100 C (the corresponding discharge time is ≈8 s) is 37.6 mA h g^{-1}, which is 63.6% of the capacity at 2 C. Considering the poor Coulombic efficiency of the $LiMn_2O_4$ cathode at low current rates cause by oxygen evolution reaction (Figure S10 in the Supporting Information), the voltage window at low current densities (i.e., 2 and 5 C was confined at 0–2.1 V (Figure 4c and Figure S9b in the Supporting Information), thus resulting in lower capacities and Coulombic efficiencies than those obtained at 10 C.

Finally, the specific power and energy of PNFE//$LiMn_2O_4$ ARLIBs were summarized and compared with representative records of aqueous lithium- and sodium-ion batteries reported previously (Figure 4d). A specific power of ≈12 610 W kg^{-1} is obtained at an energy density of ≈30.8 W h kg^{-1} (upper arrow), and still remains at ≈1838 W kg^{-1} when the specific energy increases to ≈76.1 W h kg^{-1} (lower arrow). Compared with the state-of-the-art aqueous rechargeable alkali-ion batteries, such as VO_2//$LiMn_2O_4$,[30] $LiTi_2(PO_4)_3$//$LiMn_2O_4$,[4] MoO_3@polypyrrole//$LiMn_2O_4$,[5] $LiTi_2(PO_4)_3$//$LiFePO_4$,[1] (polyaniline/Fe_2O_3)//$LiMn_2O_4$,[24] active carbon//$LiMn_2O_4$,[31] $NaTi_2(PO_4)_3$//$Na_2NiFe(CN)_6$,[32] and $NaTi_2(PO_4)_3$//$Na_2CuFe(CN)_6$,[33] our PNFE//$LiMn_2O_4$ ARLIB holds a top-level performance in energy density, power density, and cycling life (Table S3 in the Supporting Information). This performance is also superior than that of polyaniline single-walled-CNT sponge-based supercapacitor,[34] and close to that of ultrafast alkaline rechargeable Ni/Fe battery.[35]

High theoretical specific power and safety are the two main factors making ARLIBs superior to conventional organic Li-ion batteries. Nonetheless, the low voltage window and limited specific energy induced by water splitting predominately restrict the battery practical performances. The approach of using highly concentrated organic Li^+ salt-based aqueous electrolytes can expand the voltage window, but it is hard to achieve high power density by this method.[8] In our strategy, the increases of the voltage window and the energy density, while extremely high power density is maintained, are realized by passivation of the HER activity of active electrode materials. This passivation still exhibits a significant effect at a low current rate of 0.2 C, indicating the excellent chemical stability of our anodes. In addition, the conformal coating and passivation of conductive substrates is also highly important for the inhibition of hydrogen evolution and improvement of the conductivity of active materials. Thus, ARLIBs with a wider voltage window, higher energy densities, outstanding specific power and excellent cycling performance are simultaneously realized.

As a new type of anode for aqueous alkali-ion batteries, PIs have very recently attracted attention.[17,26] However, the influence of the PI structures to electrochemical hydrogen evolution, which is the critical bottleneck to ARLIBs, has still remained undiscovered, let alone the further substantial passivation via Li^+ association during charging. Although the redox potential range of PNFE/CNT network cannot fully cover its stable window before HER onset, this passivation still shows a new strategy to push the voltage window of ARLIBs. Their water splitting catalytic activity, redox potential, and Li^+ storage capability can be tuned via the design of the molecular structures.[12] Thus, PIs represent a series of promising candidates for ARLIBs with much improved energy and power. Development of new organic materials with similar structures of PIs but lower content of hydrogen binding sites (e.g., only two O atoms per unit) may serve as an approach to better passivation of water reduction.

In summary, we have discovered the passivated HER activity of PNFE/CNT networks and further developed their high performance as anodes for ARLIBs. DFT calculations predict that PNFE possesses an intrinsic sluggish activity for HER catalysis due to their large activation barrier of 2.11 eV for HER, and the Li^+ association during charging can further reduce the active sites and increase the hydrogen-evolution overpotentials. With the rational design of electrode structure, capability of HER passivation and the capacitor-like Li^+ storage kinetics, the PNFE/CNT networks exhibit a large hydrogen-evolution onset overpotential of 820 mV versus RHE, outstanding reversible capacity of 153.7 mA h g^{-1}, and ultrafast rate capability as fast as 13.6 s per charge–discharge cycle. When combined with $LiMn_2O_4$ as cathode, the PNFE//$LiMn_2O_4$ full-cell ARLIB offers a wide voltage window (>2.0 V), high specific capacity of 68.8 mA h g^{-1} at the charge and discharge current densities of 10 C, excellent energy density (76.1 W h kg^{-1}) and power density (12 610 W kg^{-1}), and extraordinary cycling stability (65.5% capacity retention after 1000 cycles when fast operated within 5 min), well exceeding most of aqueous energy-storage devices reported previously. Further design optimization of new molecular structures of PIs will lead to a promising avenue for new generation ARLIBs with much higher specific energy and power.

Supporting Information

Supporting Information is available from the Wiley Online Library or from the author.

Acknowledgements

Y.W., X.C., and Y.Z. contributed equally to this work. The authors thank the following funding agencies for supporting this work: the National Key Basic Research Program of China (2013CB934104), the Natural Science Foundation of China (21322311, 21473038), the Science and

ADVANCED MATERIALS

www.advmat.de

Chemical-to-Electricity Carbon: Water Device

Sisi He, Yueyu Zhang, Longbin Qiu, Longsheng Zhang, Yun Xie, Jian Pan, Peining Chen, Bingjie Wang, Xiaojie Xu, Yajie Hu, Cao Thang Dinh, Phil De Luna, Mohammad Norouzi Banis, Zhiqiang Wang, Tsun-Kong Sham, Xingao Gong, Bo Zhang, Huisheng Peng,* and Edward H. Sargent**

The ability to release, as electrical energy, potential energy stored at the water:carbon interface is attractive, since water is abundant and available. However, many previous reports of such energy converters rely on either flowing water or specially designed ionic aqueous solutions. These requirements restrict practical application, particularly in environments with quiescent water. Here, a carbon-based chemical-to-electricity device that transfers the chemical energy to electrical form when coming into contact with quiescent deionized water is reported. The device is built using carbon nanotube yarns, oxygen content of which is modulated using oxygen plasma-treatment. When immersed in water, the device discharges electricity with a power density that exceeds 700 mW m^{-2}, one order of magnitude higher than the best previously published result. X-ray absorption and density functional theory studies support a mechanism of operation that relies on the polarization of sp^2 hybridized carbon atoms. The devices are incorporated into a flexible fabric for powering personal electronic devices.

Converting potential energy stored at the water:material interface to electrical energy has become more and more important since water is abundant and widely available.[1–3] Recently it has been shown that the interaction between nanomaterials (such as carbon nanotubes (CNTs) or graphene) and liquids (such as water, acid solution or salt solution) can convert mechanical energy into electrical form. This enables the development of lightweight, portable, and cost-effective power sources using carbon materials and water sources.[4–6] Researchers have observed that liquid flowing through single-walled CNTs induces electric current and voltage.[7] The phenomenon was explained by the movement of the free charge carriers in the CNTs, which is appealing but resulted in an output voltage of only a few millivolts. Since then, various experiments have been designed to harvest energy from nanomaterials under liquid flow. Several mechanisms have also been proposed: for example, electricity generated by liquids driven along the surface of nanomaterials has been explained by the fluidic-electric effect,[8–10] while ionic solution flowing along graphene has been attributed to the electrokinetic phenomenon.[11,12]

Graphene oxide and porous carbon exposed to moisture have been shown to lead to electricity via the proton-transfer effect,[13,14] but these technologies were applied under water vapor which limited their range of application. Furthermore, surface charging is shown to occur when water travels past polymer nanowires.[15] However, the output of these water-based devices has not yet been improved to meet the real applications.

In summary, previously reported approaches required either carefully tuned concentrations of ionic aqueous solutions, or water to flow and interact with the nanomaterials in order to be functional.[16]

Reliance on such requirements limits electricity production from water sources widely available in nature, including remote settings and daily life. Technology that can utilize a wide range of water sources with improved output can greatly expand the

Dr. S. He, Dr. L. Qiu, L. Zhang, J. Pan, Dr. P. Chen, Dr. B. Wang, Dr. X. Xu, Y. Hu, Prof. B. Zhang, Prof. H. Peng
State Key Laboratory of Molecular Engineering of Polymers
Department of Macromolecular Science and Laboratory of Advanced Materials
Fudan University
Shanghai 200438, China
E-mail: bozhang@fudan.edu.cn; penghs@fudan.edu.cn

Dr. Y. Zhang, Y. Xie, Prof. X. Gong
Key Laboratory for Computational Physical Sciences (MOE)
State Key Laboratory of Surface Physics
Department of Physics
Fudan University
Shanghai 200433, China

Dr. C. T. Dinh, Prof. E. H. Sargent
Department of Electrical and Computer Engineering
University of Toronto
10 King's College Road, Toronto, Ontario M5S 3G4, Canada
E-mail: ted.sargent@utoronto.ca

P. De Luna
Department of Materials Science and Engineering
University of Toronto
10 King's College Road, Toronto, Ontario M5S 3G4, Canada

Dr. M. N. Banis, Dr. Z. Wang, Prof. T.-K. Sham
Department of Chemistry
University of Western Ontario
London, Ontario N6A 5B7, Canada

DOI: 10.1002/adma.201707635

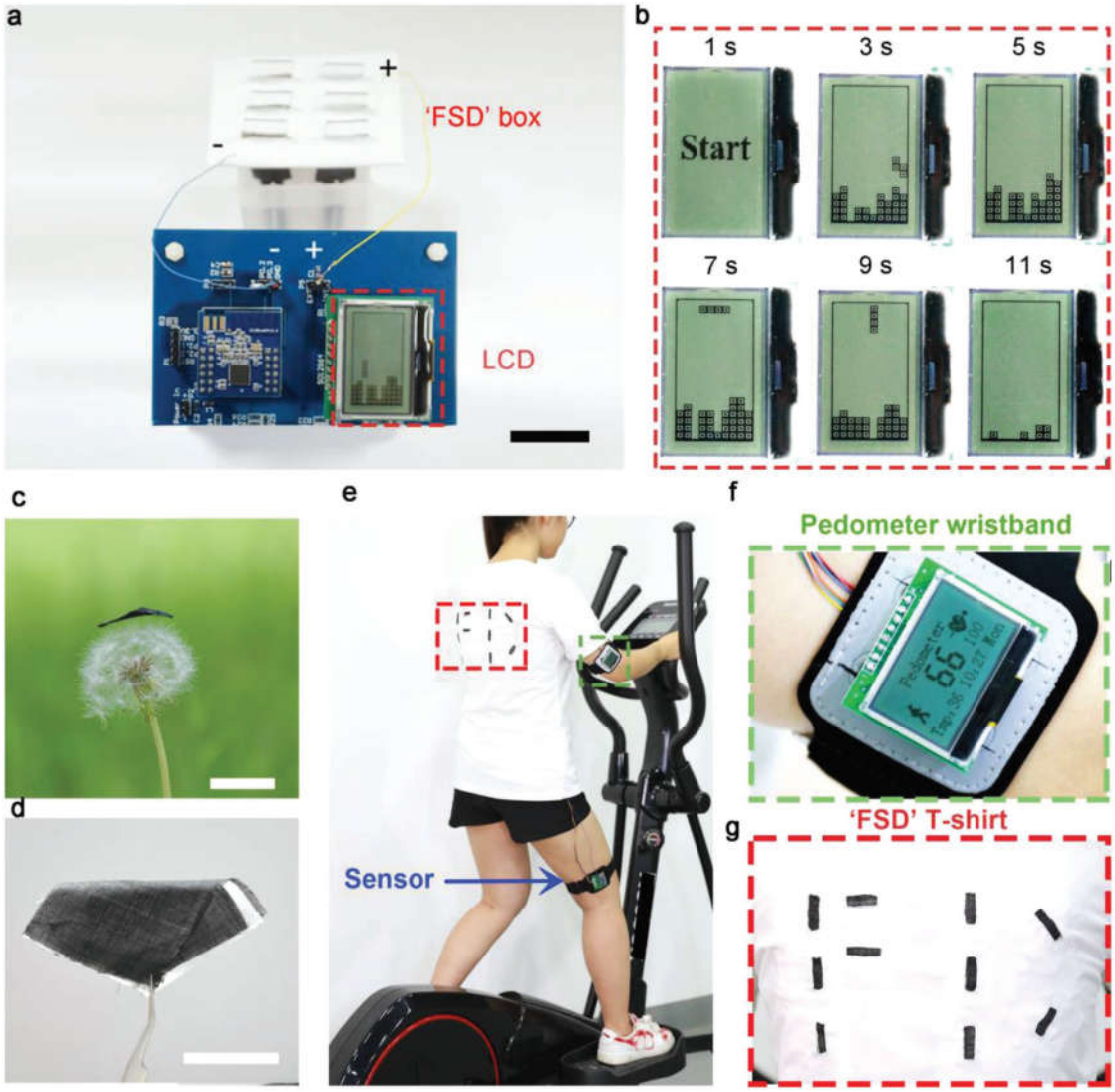

Figure 4. Energy supply application of the carbon:water device. a,b) Photographs of the liquid crystal display with movable sliding blocks powered by an "FSD" box. c) Lightweight CNT fabric on a dandelion. d) Flexible and bendable carbon:water device fabric. e) Photographs of a subject wearing an "FSD" T-shirt and a self-designed pedometer wristband during exercise on an elliptical machine. f,g) Enlarged photographs of the self-designed pedometer wristband and "FSD" T-shirt. Scale bars: 2 cm for (a), 1 cm for (c), and 2 cm for (d).

electric charge is transferred via an electrochemical reaction between CNTs and water induced by the local-polarization of OCNTs. Because our device functions in a variety of water sources and does not require flowing water or ionic solutions, it offers a new water-based electricity generation technology. Furthermore, because it is small, lightweight and flexible, the device can be made wearable and foldable in large scale. We foresee various potential applications in consumer electronics and remote emergency situations where power generation is scarce.

Supporting Information

Supporting Information is available from the Wiley Online Library or from the author.

Acknowledgements

S.H., Y.Z., L.Q., and L.Z. contributed equally to this work. This work was supported by the Ministry of Science and Technology (Grant No. 2016YFA0203302), the National Natural Science Foundation of China (Grant Nos. 21634003, 51573027, 51403038, 51673043, and 21604012), and the Science and Technology Commission of Shanghai Municipality (Grant Nos. 16JC1400702, 15XD1500400, and 15JC1490200). The sample fabrication was performed at the Fudan Nano-fabrication Laboratory. This work has also benefited from the X-ray Micro-Analysis and Spherical Grating Monochromator beamlines at Canadian Light Source. The authors thank Oleksandr Voznyy, Y. H. Wang, and G. F. Zheng for fruitful discussions and the equipment assistance, and thank X. H. Tao for the circuit design.

Conflict of Interest

The authors declare no conflict of interest.